Supplementary Information for

Enhanced ammonia synthesis activity of Ru-supported cerium-lanthanum oxide induced by Ti substitution forming mesopores

Yoshihiro Goto,*[a] Masashi Kikugawa,[a] Keisuke Kobayashi,[b] Tetsuya Nanba,[b] Hideyuki Matsumoto,[b,c] Kiyoshi Yamazaki,[a] Mitsuru Matsumoto[a] and Haruo Imagawa[a]

[a] *Toyota Central R&D Labs., Inc., 41-1 Yokomichi, Nagakute, Aichi 480-1192, Japan.*

[b] *Renewable Energy Research Center, National Institute of Advanced Industrial Science and Technology, 2-2-9 Machiikedai, Koriyama, Fukushima 963-0298, Japan.*

[c] *Department of Chemical Science and Engineering, School of Materials and Chemical Technology, Tokyo Institute of Technology, 2-12-1 Ookayama, Meguro-ku, Tokyo, 152–8552, Japan.*

1. Experimental section

1.1 Material synthesis

Solid solutions of polycrystalline $Ce_{0.5}La_{0.5-x}Ti_xO_{1.75+0.5x}$ (x = 0, 0.1, 0.2, 0.3, 0.4, and 0.5) samples were synthesized using the polymerized complex method. $Ce(NO_3)_3 \cdot 6H_2O$ (98%, FUJIFILM Wako Chemicals), $La(NO_3)_3 \cdot 6H_2O$ (99.9%, FUJIFILM Wako Chemicals), $TiO(NO_3)_2$ aqueous solution, citric acid (98%, FUJIFILM Wako Chemicals), and ethylene glycol (99%, FUJIFILM Wako Chemicals) were dissolved in a minimum amount of deionized water in a molar ratio of 0.5:(0.5−x):x:6:12. $TiO(NO_3)_2$ aqueous solution was prepared by dissolving $TiO(OH)_2$ (obtained by hydrolyzing $Ti(OC_3H_7)_4$; 95%, FUJIFILM Wako Chemicals) in a minimum amount of aqueous HNO_3 solution (65%, FUJIFILM Wako Chemicals). The resulting solution was stirred at 90 °C for 1 h to promote polymerization and then dried at 300 °C until the product became a gel. The gel was preheated at 500 °C for 10 h and calcined twice at 700 °C for 10 h in air. Cs/MgO as a benchmark compound was prepared by impregnation using MgO (0.2 μm, 99.9%, FUJIFILM Wako Chemicals) and Cs_2CO_3 (99.9%, Sigma-Aldrich)/ethanol (99.5%, FUJIFILM Wako Chemicals), followed by calcination at 500 °C for 5 h in N_2. $Ru/Ce_{0.5}La_{0.5-x}Ti_xO_{1.75+0.5x}$ and Ru-Cs/MgO were prepared by impregnation using $Ru_3(CO)_{12}$ (99%, Sigma-Aldrich)/THF (99.5%, FUJIFILM Wako Chemicals) solution. The suspension was stirred at room temperature for 6 h, and then the solvent was

evaporated under reduced pressure. The obtained compound was dried at 80 °C for 40 h and calcined at 500 °C for 5 h in N_2. The Cs and Ru loading amounts on the metal basis were 3 wt.%.1.2 Characterization

X-ray diffraction (XRD) patterns were collected on an Ultima IV X-ray diffractometer (Rigaku) using Cu Kα radiation (λ = 1.54056 Å). The collected XRD patterns were analyzed with the Le-Bail method using the program JANA2006[S1] to estimate the lattice parameters. High-angle annular dark-field scanning transmission electron microscopy (HAADF-STEM) images were collected using a Tecnai Osiris (FEI) operated at 200 kV. X-ray absorption near edge structure (XANES) spectra were recorded in transmission mode using BL33XU (Spring-8, Hyogo, Japan). The spectra of the samples in oxidizing atmosphere were collected at 50 °C in 5% O_2/He. The spectra of the reduced samples were collected at 600 °C in 5% H_2/He after a holding time of 1 h. X-ray photoelectron spectroscopy (XPS) was conducted on a PHI-5500MC instrument (ULVAC PHI) using Mg Kα radiation (1253.6 eV). The XPS binding energies were calibrated by shifting the O 1*s* peak to 529.2 eV. The spectra were collected after reduction at 600 °C in 5% H_2/He for 1 h. Nitrogen adsorption-desorption isotherms were recorded at −196 °C using a BELSORP-mini II (MicrotracBEL) after pre-treatment at 300 °C for 30 min under vacuum. CO pulse adsorption measurements were conducted on a flow-type adsorption apparatus R6015-S (HEMMI Slide Rule). The CO pulse injections were performed at −78 °C after reduction at 600 °C in 100% H_2 for 1 h.

1.3 Catalytic reaction

The ammonia synthesis reaction under atmospheric pressure was conducted in a fixed-bed reactor connected to mass flow controllers. The sample (0.2 g) was placed on a bed of quartz wool in a quartz tube and then pre-reduced at 600 °C for 1 h in a stream of H_2/N_2 = 3 gas with a flow rate of 80 mL min^{-1}. A catalytic test was conducted at 280–400 °C in a stream of H_2/N_2 = 3 gas mixture with a flow rate of 80 mL min^{-1}. High-purity gases (Taiyo Nippon Sanso JFP, H_2 99.99999%, N_2 99.99995%) were used for the pre-reduction and the catalytic test, because a gas mixture of purity over 99.9999% can maintain the long-term stability of Ce and La based catalysts.[S2] The ammonia concentration of the vent gas was monitored by Fourier-transform infrared (FT-IR) spectroscopy and converted into an ammonia synthesis rate. The ammonia synthesis reaction under high pressure was conducted in a high-pressure reactor connected to mass flow controllers. The sample (1.0 g) was placed on a bed of quartz wool in a stainless tube and then pre-reduced at 600 °C for 1 h in a stream of H_2/N_2 = 3 gas mixture with a flow rate of 400 mL min^{-1}. Catalytic tests were conducted at 320 °C and 0–5 MPaG (gauge pressure) in a stream of H_2/N_2 (ratio = 0.5–3 gas) with a flow rate of 400 mL min^{-1}. The ammonia synthesis rate was estimated in the same way as the reaction at atmospheric pressure.

1.4 Kinetic analysis

The reaction orders for the ammonia synthesis reaction were determined by the method reported by Aika et al.[S3] Technically, reaction orders with respect to H_2 (h) and N_2 (n) were estimated from H_2 and N_2 partial pressure dependences, respectively, for the ammonia synthesis rate (r) given by equation (1). The reaction order with respect to NH_3 (a) was estimated from the total flow rate dependence of the ammonia synthesis rate. The reaction conditions and ammonia synthesis rates are listed in Table S1. The typical ammonia concentration is far from the thermodynamic equilibrium (the maximum yield is approximately 11% to the equilibrium value). The synthesis rates were analyzed based on equations (2)–(5), and the reaction orders were obtained (Fig. S5 and Table S2).

$$r = kP_{H_2}^{h} P_{N_2}^{n} P_{NH_3}^{a} \quad (1)$$

$$r = \left(\frac{1}{w}\right)\frac{dy_0}{d(1/q)} \quad (2)$$

$$\log y_0 = \log\left(\frac{C}{q}\right)^{\frac{1}{m}} \quad (3)$$

$$r = \left(\frac{1}{w}\right)\left(\frac{C}{m}\right) y_0^{(1-m)} \quad (4)$$

$$C = k_2 P_{H_2}^{h} P_{N_2}^{n} \quad (5)$$

r, w, y_0, q, and $(1 - m)$ represent the ammonia synthesis rate, catalyst weight, ammonia mole fraction at the reactor outlet, total flow rate, and a (reaction order with respect to NH_3), respectively, while k, k_2, and C are constants.

2. Supplementary figures

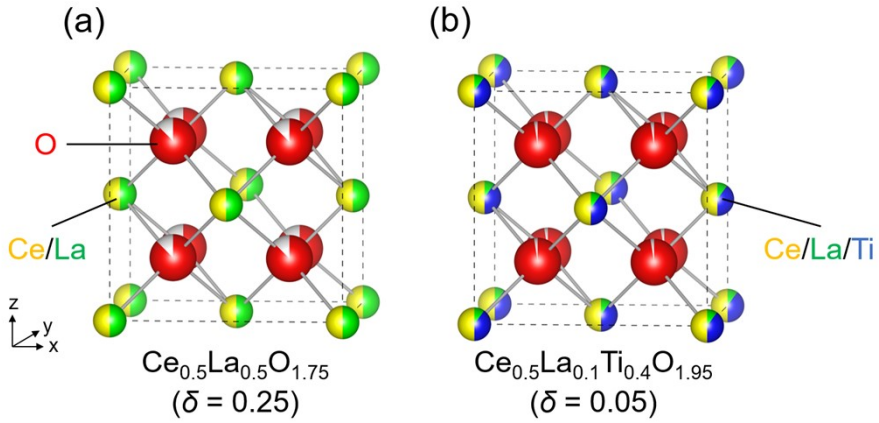

Fig. S1. Crystal structures of (a) $Ce_{0.5}La_{0.5}O_{1.75}$ and (b) $Ce_{0.5}La_{0.1}Ti_{0.4}O_{1.95}$ with the $AO_{2-\delta}$ fluorite structure (space group *Fm*-3*m*). The yellow, green, blue, and red spheres represent Ce, La, Ti, and O, respectively. The crystal structures are depicted by VESTA.[S4]

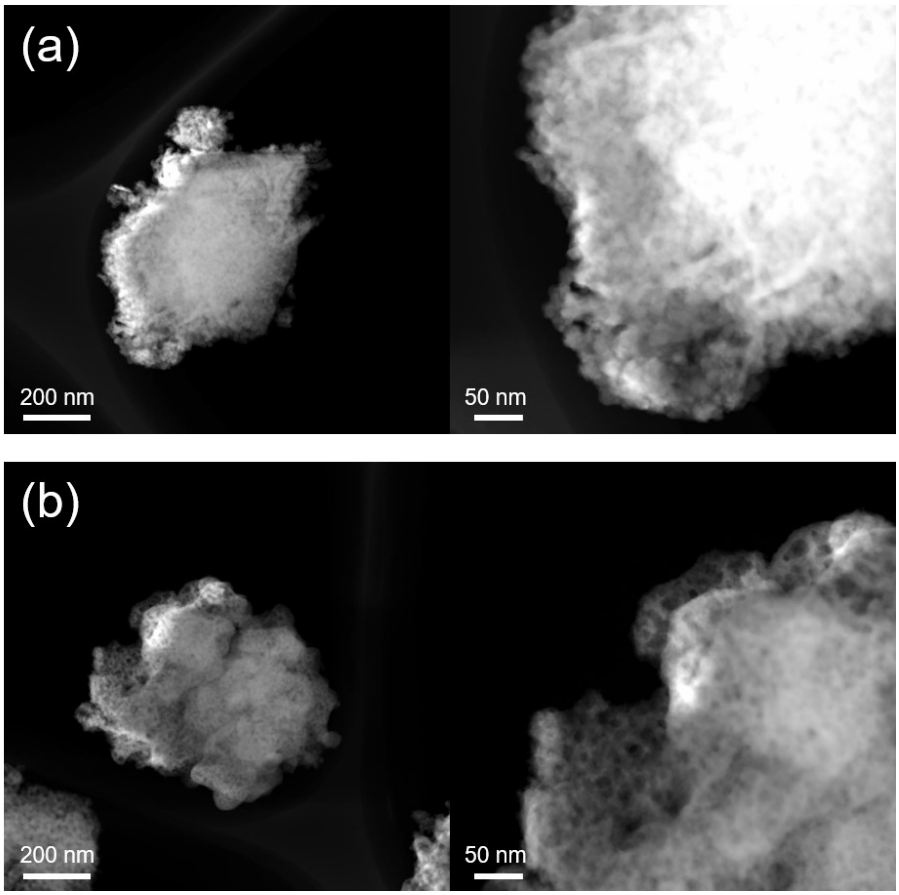

Fig. S2. HAADF-STEM images of (a) $Ru/Ce_{0.5}La_{0.5}O_{1.75}$ and (b) $Ru/Ce_{0.5}La_{0.4}Ti_{0.1}O_{1.8}$.

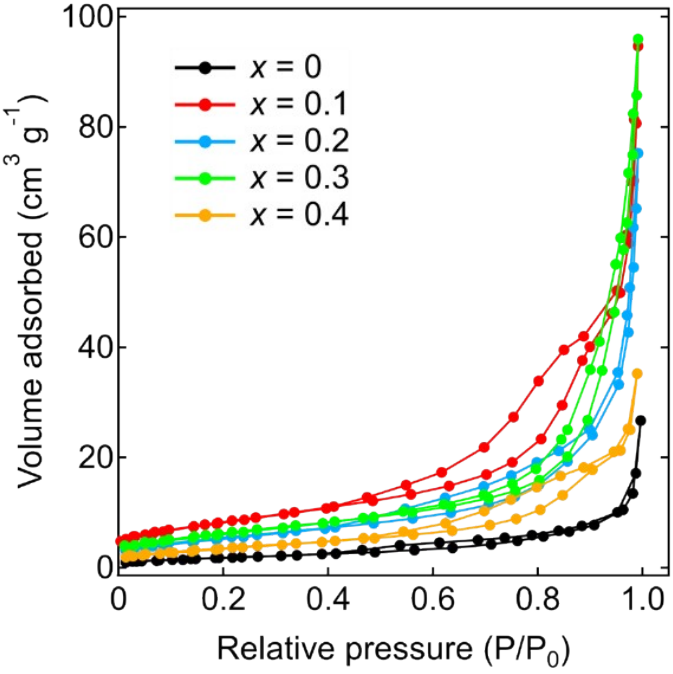

Fig. S3. Nitrogen adsorption-desorption isotherms of $Ru/Ce_{0.5}La_{0.5-x}Ti_xO_{1.75+0.5x}$ ($0 \leq x \leq 0.4$).

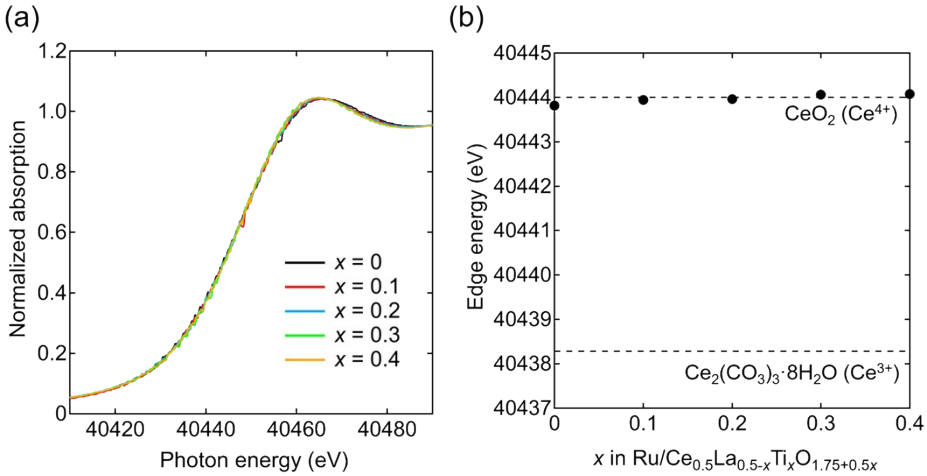

Fig. S4. (a) Ce K-edge XANES spectra and (b) edge energy of $Ru/Ce_{0.5}La_{0.5-x}Ti_xO_{1.75+0.5x}$ ($0 \leq x \leq 0.4$) at 50 °C in 5% O_2/He.

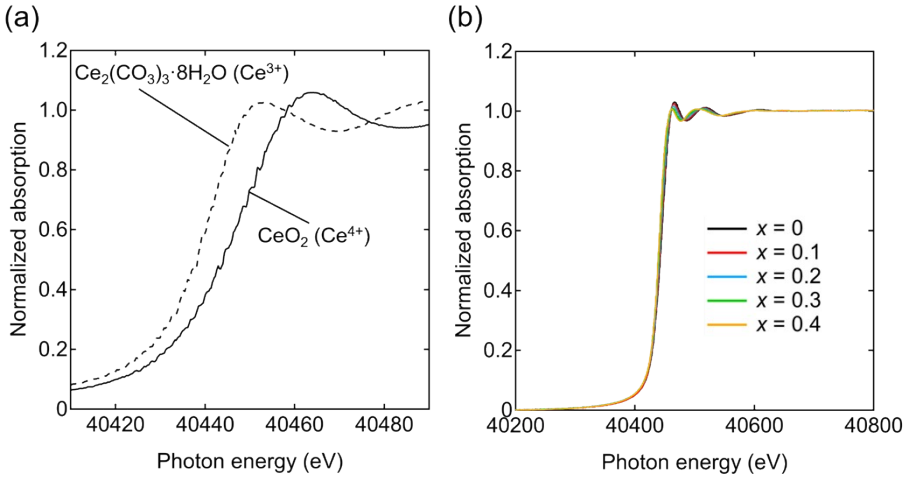

Fig. S5. Ce K-edge XANES spectra of (a) $Ru/Ce_{0.5}La_{0.5-x}Ti_xO_{1.75+0.5x}$ ($0 \leq x \leq 0.4$) at 600 °C in 5% H_2/He and (b) CeO_2 (Ce^{4+}) and $Ce_2(CO_3)_3 \cdot 8H_2O$ (Ce^{3+}) references at room temperature in air.

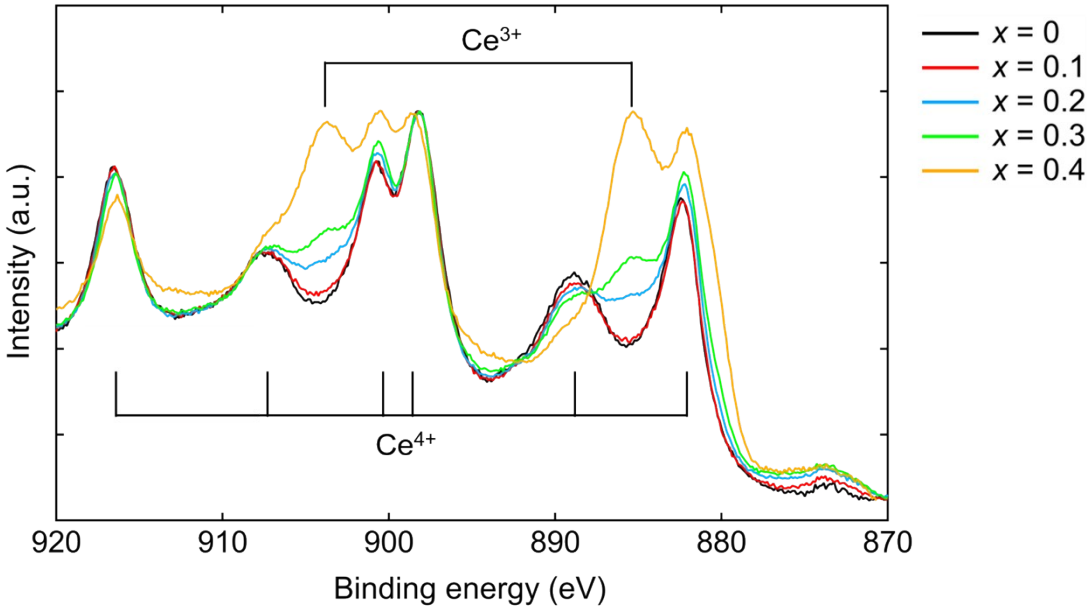

Fig. S6. Ce 3*d* XPS spectra for Ru/$Ce_{0.5}La_{0.5-x}Ti_xO_{1.75+0.5x}$ ($0 \leq x \leq 0.4$) after pre-reduction at 600 °C in 4% H_2/Ar for 1 h.

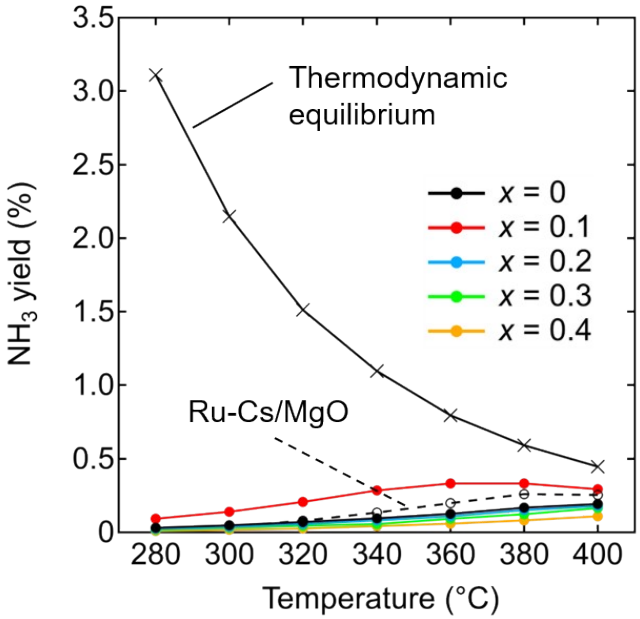

Fig. S7. Temperature dependence of NH_3 yields for $Ru/Ce_{0.5}La_{0.5-x}Ti_xO_{1.75+0.5x}$ ($0 \leq x \leq 0.4$) and Ru-Cs/MgO.

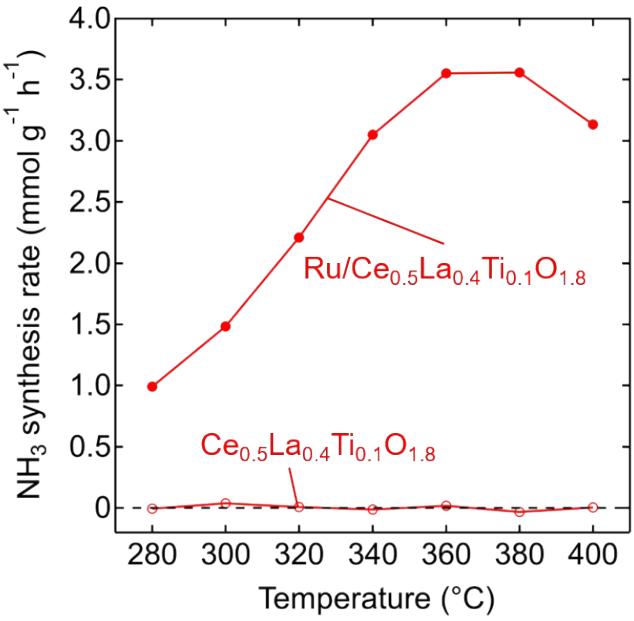

Fig. S8. Temperature dependence of NH_3 synthesis rate for $Ce_{0.5}La_{0.4}Ti_{0.1}O_{1.8}$ with and without Ru-loading.

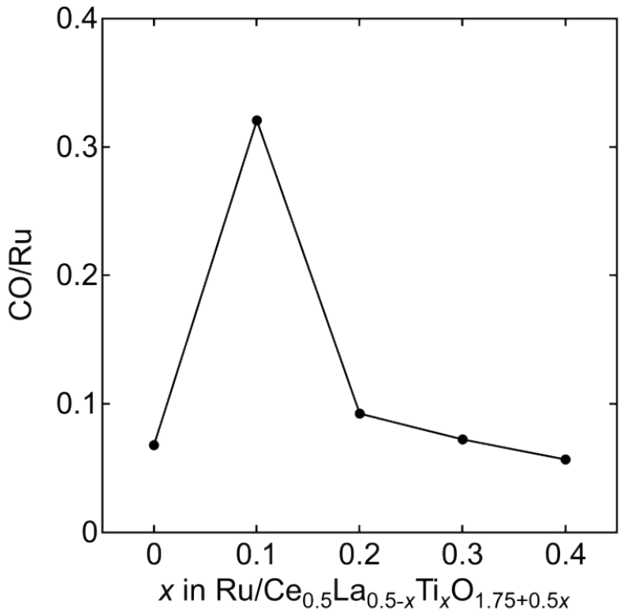

Fig. S9. CO/Ru ratios of $Ru/Ce_{0.5}La_{0.5-x}Ti_xO_{1.75+0.5x}$ ($0 \leq x \leq 0.4$).

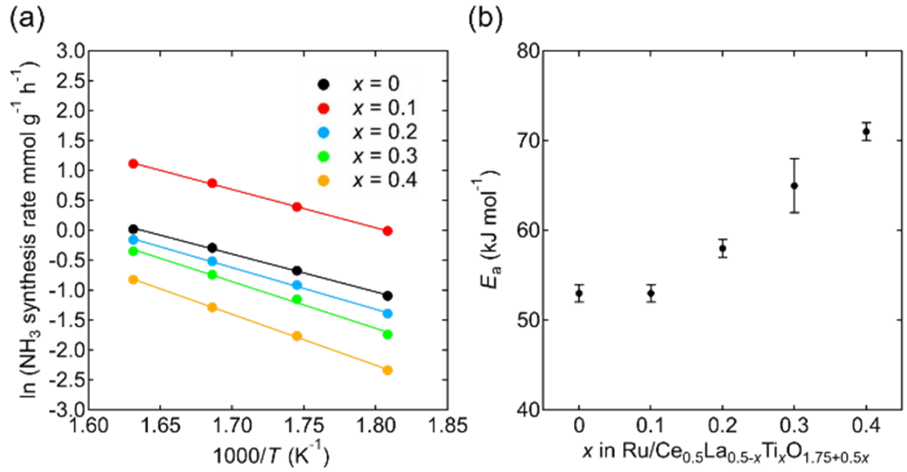

Fig. S10. (a) Arrhenius plots and (b) activation energy for NH_3 synthesis rates of Ru/$Ce_{0.5}La_{0.5-x}Ti_xO_{1.75+0.5x}$ ($0 \leq x \leq 0.4$).

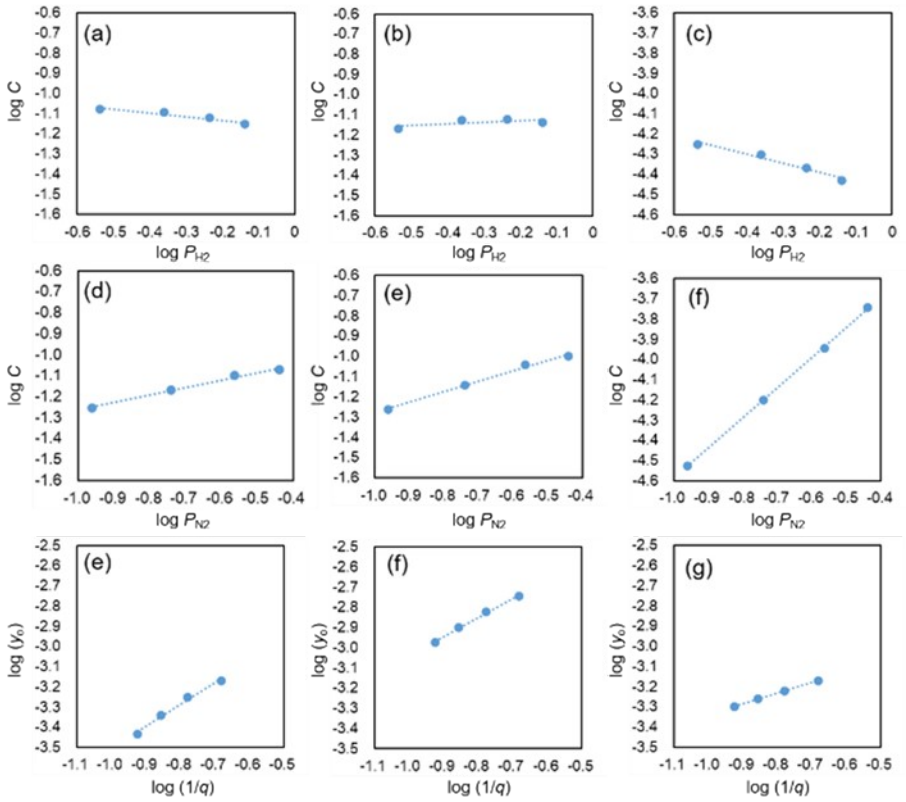

Fig. S11. Dependence of H_2 partial pressure (a−c), N_2 partial pressure (d−f), and flow rate (e−g) on ammonia synthesis rates of $Ru/Ce_{0.5}La_{0.5}O_{1.75}$ (a, d, e), $Ru/Ce_{0.5}La_{0.4}Ti_{0.1}O_{1.8}$ (b, e, f), and Ru-Cs/MgO (c, f, g) at 320 °C and 0.1 MPa. The synthesis rates were obtained under the reaction conditions listed in Table S1. Reaction orders with respect to H_2, N_2, and NH_3 (Table S2) were estimated by the equation described in the experimental section.

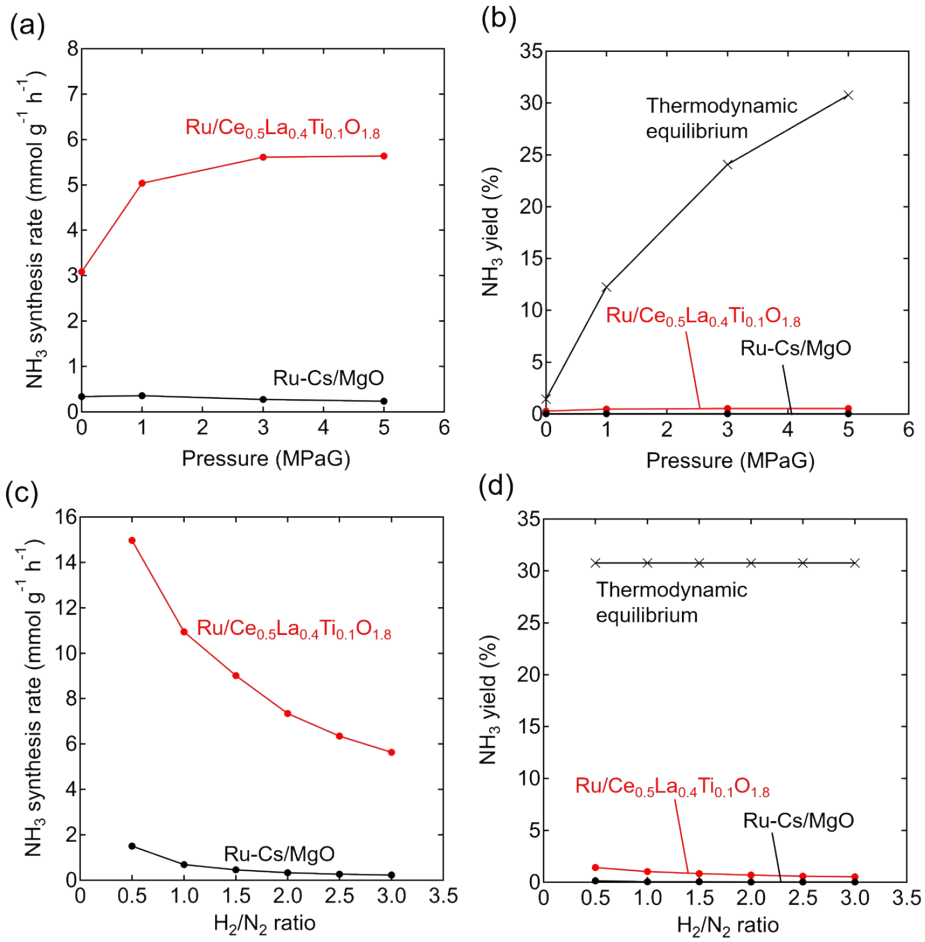

Fig. S12. Pressure dependence on (a) NH_3 synthesis rate and (b) NH_3 yields of $Ru/Ce_{0.5}La_{0.4}Ti_{0.1}O_{1.8}$ (x = 0.1) and Ru-Cs/MgO at 320 °C and H_2/N_2 = 3. Influence of H_2/N_2 ratio in the feed gas on (c) NH_3 synthesis rate and (d) NH_3 yields at 320 °C and 5 MPaG. (Reaction conditions: catalyst, 1.0 g; flow rate, 400 mL min^{-1})

3. Supplementary tables

Table S1. Reaction conditions[a] and ammonia synthesis rates for kinetic analysis.

Reaction order	H_2/N_2 ratio	Flow rate (mL min^{-1})				NH_3 synthesis rate/Yield to Yield-eq. (mmol g^{-1} h^{-1})/(%)		
		H_2	N_2	Ar	Total	$Ru/Ce_{0.5}La_{0.5}O_{1.75}$	$Ru/Ce_{0.5}La_{0.4}Ti_{0.1}O_{1.8}$	Ru-Cs/MgO
H_2	2	32	16	62	110	0.60/2.8	1.32/6.1	0.67/3.1
	3	48	16	46	110	0.58/2.6	1.44/6.5	0.63/2.9
	4	64	16	30	110	0.54/2.5	1.45/6.6	0.58/2.7
	5	80	16	14	110	0.50/2.4	1.41/6.7	0.54/2.6
N_2	5	60	12	38	110	0.39/1.9	2.15/5.1	0.48/2.3
	3	60	20	30	110	0.48/2.2	2.79/6.3	0.71/3.2
	2	60	30	20	110	0.57/2.7	3.46/8.1	0.97/4.5
	1.5	60	40	10	110	0.61/3.1	3.79/9.5	1.24/6.2
NH_3	3	48	16	16	80	0.66/4.1	1.75/10.9	0.66/4.1
	3	60	20	20	100	0.68/3.4	1.83/9.1	0.73/3.7
	3	72	24	24	120	0.67/2.8	1.84/7.7	0.80/3.3
	3	84	28	28	140	0.63/2.3	1.81/6.4	0.86/3.1

[a] All data were collected at 320 °C and atmospheric pressure (the maximum yield is approximately 11% to the equilibrium value).

Table S2. Reaction orders[a] for ammonia synthesis reaction over different catalysts

Catalyst	Order		
	H_2	N_2	NH_3
$Ru/Ce_{0.5}La_{0.5}O_{1.75}$	−0.18	0.35	0.07
$Ru/Ce_{0.5}La_{0.4}Ti_{0.1}O_{1.8}$	0.08	0.51	−0.07
Ru-Cs/MgO	−0.45	1.50	−0.91

[a] Estimated from results of kinetic analysis shown in Fig. S10.

4. References

S1 V. Petříček, M. Dušek and L. Palatinus, *Z. Kristallogr. - Cryst. Mater.*, 2004, **229**, 345.

S2 K. Sato, S. Miyahara, Y. Ogura, K. Tsujimaru, Y. Wada, T. Toriyama, T. Yamamoto, S. Matsumura and K. Nagaoka, *ACS Sustainable Chem. Eng.*, 2020, **8**, 2726.

S3 K. Aika, M. Kumasaka, T. Oma, O. Kato, H. Matsuda, N. Watanabe, K. Yamazaki, A. Ozaki and T. Onishi, *Appl. Catal.* 1986, **28**, 57.

S4 K. Momma and F. Izumi, *J. Appl. Crystallogr.*, 2011, **44**, 1272.